Modeling Water Absorption in Wood with an Improved Approximation Method

Samuel V. Glass, PhD
Member ASHRAE

Charles R. Boardman
Member ASHRAE

Eleanor Q. Daniels

ABSTRACT

Combined heat and moisture transfer modeling is used in building envelope analysis to identify potential moisture durability risks. Moisture transfer in porous materials is typically partitioned into liquid transport and vapor diffusion. Although modeling approaches differ in complexity, coefficients for liquid transport are often derived from laboratory measurements of water absorption by partial immersion. Models generally include the assumption that capillary transport is dominant during the measurement, while vapor diffusion is negligible. This is reasonable for mineral-based materials, but recent work indicates that it may be incorrect for wood. This paper builds on earlier work and develops an improved approximation method for liquid diffusivity in wood from water absorption measurements. The approach does not require additional data beyond ordinary hygrothermal property measurements, and it partitions vapor and liquid transport in a practical way that is guided by current understanding of wood–water interactions. The improved liquid diffusivity approach is calibrated using one-dimensional simulations compared with measured water uptake in a range of wood species from the literature.

1. INTRODUCTION

The building envelope performs multiple functions that are critical for comfortable, healthy, energy efficient, and durable buildings. Among these are control of bulk water, water vapor flow, airflow, and heat flow. Excessive moisture in buildings can lead to health problems and deterioration of building materials. Simulation of moisture and temperature conditions within a building assembly in response to environmental loads is an important tool for design and forensic analysis.

Porous building materials absorb water by capillary action. Water absorption may occur in various ways: cladding materials exposed to wind-driven rain; materials in contact with wet ground; or materials exposed to weather during the construction process. A common laboratory method for measuring liquid water absorption is by partial immersion (ASTM 2019; ISO 2002). The sides of the specimen are sealed with a water-impermeable coating to limit absorption to one surface and the specimen is immersed in water to a depth of a few millimeters, periodically removed, weighed, and immersed again. In many cases a plot of water uptake ($kg \cdot m^{-2}$ or $lb \cdot ft^{-2}$) versus square root of time is linear, and the slope of the plot gives the water absorption coefficient, A ($kg \cdot m^{-2} \cdot s^{-0.5}$ or $lb \cdot ft^{-2} \cdot h^{-0.5}$).

Hygrothermal models typically partition moisture transfer in building materials into two mechanisms: vapor diffusion and liquid transport. It is generally assumed that liquid transport is dominant during a water absorption experiment and vapor diffusion is negligible in comparison. Models for liquid diffusivity in porous materials range from simplified approximations (Kumaran 1999) that rely only on A and w_c, the capillary saturation (or free water saturation) value ($kg \cdot m^{-3}$ or $lb \cdot ft^{-3}$), to more detailed models (Carmeliet et al. 2007) with up to eight parameters that describe transport as a function of water content. For this detailed approach, measurements beyond A and w_c are needed, including water content profiles as a function of time during the absorption process and a drying experiment.

S.V. Glass is a Research Physical Scientist, **C.R. Boardman** is a General Engineer, and **E.Q. Daniels** is a Physical Science Technician in the Building and Fire Sciences Unit, USDA Forest Products Laboratory, Madison, WI, USA.

WUFI software (**W**ärme **U**nd **F**euchte **I**nstationär or "transient heat and moisture transfer"; IBP 2021) includes vapor diffusion and liquid transport. For the latter, it uses an approximation developed by Künzel (1995), where the liquid transport coefficient for suction D_w ($m^2 \cdot s^{-1}$ or $ft^2 \cdot h^{-1}$) as a function of water content w ($kg \cdot m^{-3}$ or $lb \cdot ft^{-3}$) is calculated as

$$D_w(w) = 3.8\left(\frac{A}{w_c}\right)^2 1000^{w/w_c - 1} \tag{1}$$

This approximation yields reasonable agreement between simulations and measurements for natural stone materials, both for water uptake vs. square root of time and water content profiles at different times during the absorption process (Krus 1996).

Equation (1) has been applied to many materials in the WUFI North America Database (IBP 2021), based on laboratory measurements from Kumaran et al. (2002), which included five wood species, with the default assumption that liquid transport begins at 80% relative humidity. At a basic level, when hygrothermal properties are implemented in a model, the model should be able to reproduce the measurements using the same boundary conditions as the laboratory. However, recent work indicates that Equation (1) may be inaccurate for modeling water absorption in wood (Kordziel et al. 2020). For illustration, the simulated water absorption tests using properties for spruce and eastern white cedar from the WUFI North America Database are compared with the laboratory measurements reported by Kumaran et al. (2002) in Figure 1. In both cases the simulations overpredict the rate of water uptake compared with measured data and indicate that vapor diffusion is not negligible. These examples highlight the need to create independent models for wood and mineral-based materials.

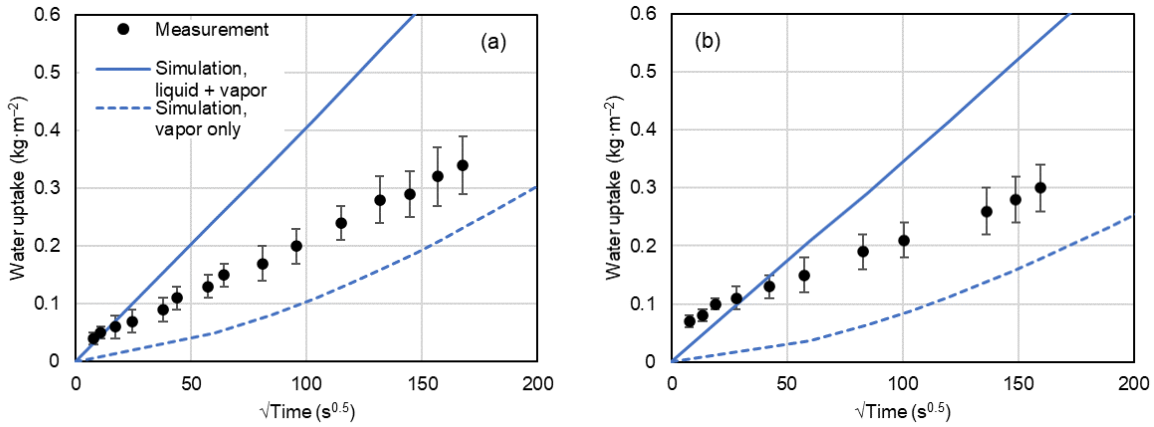

Figure 1 Water absorption measurements (Kumaran et al. 2002) for (a) spruce and (b) eastern white cedar compared with simulations using properties for the same materials from the WUFI North America Database, with and without liquid transport. Vapor diffusion is modeled using Fickian equations.

Wood responds to water differently than mineral-based materials. Wood expands and contracts with changes in moisture content. Transport properties in wood depend on the orientation relative to the growth rings and the axial direction of the tree. In some instances, liquid water uptake vs. square root of time is non-linear (Zillig 2009; Sedighi-Gilani et al. 2012; Zelinka et al. 2016). Although water vapor sorption in wood cell walls and the combined transport of water vapor in cell voids plus hygroscopic water in the cell walls is often modeled as a single Fickian diffusion process for building-scale applications, at small length scales, Fickian diffusion models break down (Thybring et al. 2019). Despite these complexities, an approximation for practical engineering analysis is still desirable.

The objective of this paper is to develop an improved approximation method for liquid water absorption that is applicable to a range of wood species, does not require additional data beyond ordinary hygrothermal property measurements, avoids the incorrect assumption that vapor diffusion is negligible during liquid water uptake measurements,

addresses the partitioning of vapor and liquid transport, and is informed by current understanding of wood–water interactions.

2. BACKGROUND ON WATER IN WOOD

Wood cell walls are composed of ordered cellulose, amorphous cellulose, hemicelluloses, and lignin. Water molecules interact with the hydroxyl (-OH) groups of these polymers through hydrogen bonding (Chen et al. 2018, Plaza 2019). Water molecules increase the volume of the cell wall, which is reflected in macroscopic swelling and shrinkage of wood with changes in moisture content. We refer to this type of water as cell wall water (the term "bound water" is also frequently used). Cell wall water does not undergo a phase change at temperatures as low as –65 °C (–85 °F) based on differential scanning calorimetry (DSC) measurements (Zelinka et al. 2012). In contrast to cell wall water, capillary water within the pore structure of wood does undergo a freezing/melting transition.

The moisture storage function describes the relationship between equilibrium moisture content and relative humidity (RH) across the hygroscopic and over-hygroscopic range. Moisture content (MC) here refers to the mass of water expressed as a percentage of dry solid mass (water content expressed in $kg \cdot m^{-3}$ or $lb \cdot ft^{-3}$ can be calculated from MC and bulk wood density). The total amount of water in wood increases dramatically at high RH, as shown in Figure 2. Measurements in softwoods indicate that this increase is primarily from cell wall water up to RH levels above 99%; in most cases the amount of capillary water is negligible below 99% RH (Thygesen et al. 2010; Fredriksson 2019). For example, DSC measurements did not detect any capillary water in Douglas-fir equilibrated at 95% RH, and at 99.65% RH the amount of capillary water was less than 0.4% MC (Fredriksson and Thybring 2019). Calculations based on softwood anatomical features (bordered pits and the pointed ends of tracheids) predict a contribution from capillary water of about 0.01% MC at 99% RH, increasing to just under 0.35% MC at 99.9% RH (Engelund et al. 2010). This value at 99.9% RH is roughly consistent with the measurements quoted above. As RH increases above 99.9%, the amount of capillary water increases rapidly, corresponding to filling of the pore structure.

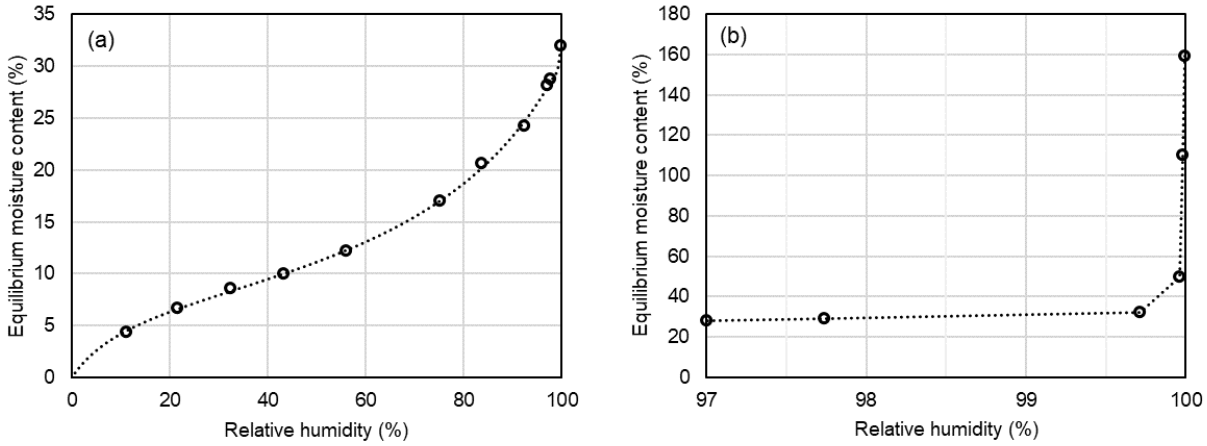

Figure 2 Sorption data for loblolly pine (Zhang and Peralta 1999), measured in desorption at 30 °C (86 °F): (a) hygroscopic range and (b) over-hygroscopic range. Note the different horizontal and vertical axis scales. Dotted lines serve only to guide the eye.

While mineral-based materials often reach capillary saturation within a practical amount of time after starting a partial immersion test, this is not the case for water uptake in wood. Although maximum saturation can be measured readily under vacuum or pressure, this value generally exceeds the free capillary saturation value because of entrapped air within the pore structure. Several studies have measured moisture profiles in wood during water absorption with techniques such as gamma ray attenuation, nuclear magnetic resonance (NMR), neutron radiography, and X-ray computed tomography. These methods

yield capillary saturation values for softwoods typically in the range 150–200% MC or 650–900 kg·m^{-3} (40–56 lb·ft^{-3}) (Krus and Vik 1999; Kumaran 1999; Sandberg and Salin 2012; Sedighi-Gilani et al. 2012; Gezici-Koç et al. 2017). A notable finding of NMR is that the cell wall water content rises spatially through the specimen before capillary water uptake (Gezici-Koç et al. 2017).

Water vapor transmission through wood increases with increasing relative humidity. The vapor permeability and vapor diffusion resistance factor for select wood species are plotted in Figure 3. Vapor diffusion resistance factor (or μ-value) is the ratio of the vapor permeability of still air (diffusion with no convection) to that of the material. These trends reflect the increase in mobility of cell wall water with increasing RH. The primary pathway is diffusion of water vapor through the pore structure, but this usually does not provide a continuous path. Molecules must cross the cell wall (or pass through bordered pits or other features) to get to the next void. As RH increases, the cell wall water content increases, which swells the cell wall, increases its porosity and the connectivity of water molecules (Kulasinski et al. 2015), and softens the amorphous polymers (Jakes et al. 2019). Additionally, the strength of attraction between water and cell wall polymers decreases as RH increases (Nopens et al. 2019), thereby increasing water mobility.

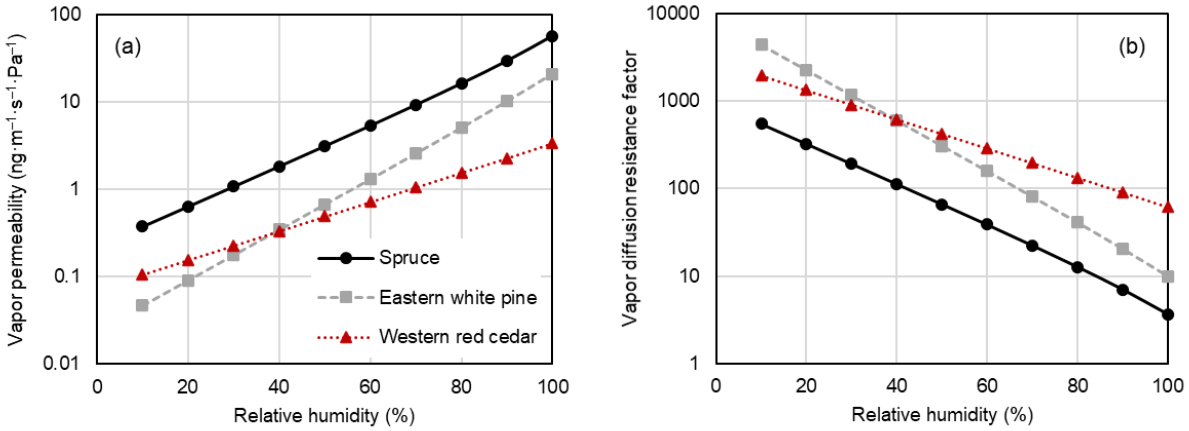

Figure 3 Semi-log plots of (a) vapor permeability vs. RH for three woods (Kumaran et al. 2002) and (b) calculated vapor diffusion resistance factor vs. RH.

3. DEVELOPMENT OF AN IMPROVED APPROXIMATION FOR LIQUID DIFFUSIVITY

The aim of this paper is to develop an improved model for liquid transport that is applicable to a range of wood species. Model predictions ought to agree with measurements, and the model framework should be consistent with the fundamental physics covered in the previous section. Our preference is to limit the number of model parameters and to use material property inputs that are readily available. Although Kordziel et al. (2020) found that Equation (1) could be empirically modified to give agreement between simulations and measurements, they did not consider the fundamental physics.

Our approach was informed by an interlaboratory study of water uptake in wood summarized by Kumaran (1999). Matched wood specimens were studied with advanced measurement and analysis methods, but different laboratories arrived at liquid diffusivity functions having highly dissimilar shape and magnitude. Kumaran (1999) suggested that a simple constant diffusivity, independent of water content, would be suitable to approximate the behavior for practical analysis:

$$D_w \approx \left(\frac{A}{w_c}\right)^2 \tag{2}$$

This equation served as a starting point. Based on the previous section, we selected water content at 99% RH as the threshold

for liquid transport and used an RH-dependent water vapor diffusion resistance factor, or μ-value, up to 90% RH. We made the μ-value constant between 90% and 100% RH because water vapor transmission measurements are rarely made above a mean RH of 90% (which corresponds to wet cup at 100% RH and chamber at 80% RH), making extrapolation above this value uncertain.

The relatively slow uptake of water in wood perpendicular to grain, together with the observation that vapor diffusion is not negligible in simulations (Figure 1), implies that the experimentally measured A-value reflects both liquid and vapor transport. In our framework, vapor transport (with RH-dependent μ-value) includes diffusion of water vapor in the pore structure coupled with diffusion of cell wall water. If the liquid diffusivity is calculated from the experimental A-value and the simulation separately includes vapor transport, the simulation would effectively be double counting the vapor diffusion contribution. This explains the overprediction in Figure 1. Therefore, we modified Equation (2) by subtracting a term that represents vapor diffusion, which is expected to be proportional to the reciprocal of the μ-value:

$$D_w = k_1 \left(\frac{A}{w_c}\right)^2 - \frac{k_2}{\mu(90)} \tag{3}$$

where $\mu(90)$ is the vapor diffusion resistance factor at 90% RH and k_1 and k_2 are fitting parameters. The value of k_1 is expected to be close to 1, although Kumaran (1999) provided another equation attributed to Krus and Künzel (1993) where $D_w = (\pi/4)(A/w_c)^2$. In the next section we describe how the fitting parameters are optimized.

4. METHODS

Measured water absorption data and other hygrothermal property data for various wood species were obtained from three literature sources (the term "species" here refers to commercial groups rather than strict botanical taxonomy):

1. Kumaran et al. (2002): eastern white cedar, western red cedar, eastern white pine, southern yellow pine, and spruce
2. Zelinka et al. (2016): southern yellow pine with transport in the radial and tangential directions
3. Kordziel et al. (2020): spruce-pine-fir group and Douglas-fir

Capillary saturation was not measured in the first two sources. The WUFI Database relies on an extrapolation to approximate capillary saturation based on the data of Kumaran et al. (2002). Zelinka et al. (2016) extrapolated w_c from the water uptake vs. time curve with a kinetic model. Neither extrapolation method consistently yielded w_c values within the range of literature values described in Section 2. Instead, we estimated capillary saturation as 90% of the measured maximum saturation value, which yielded w_c values within the expected range. In some cases, the porosity input value needed to be increased to allow an increase in w_c, but porosity had no direct effect on the model.

The moisture storage function for the five wood species of Kumaran et al. (2002) was also modified in the high RH range to better align with the literature. In the WUFI database, linear interpolation is used between one data point at about 89% RH and another value from pressure plate data at 99.78%–99.92% RH, as shown in Figure 4. This interpolation does not correctly represent the shape of the moisture storage function in comparison to more detailed measurements. Based on literature data for North American softwoods (Stone and Scallan 1967; Fortin 1979; Tremblay et al. 1996; Zhang and Peralta 1999; Wang et al. 2014), the following estimated RH/EMC pairs were inserted for spruce and the two pine species: (95% RH, 26% MC); (98% RH, 30% MC); (99% RH, 35% MC); and (99.6% RH, 50% MC). Cedar is known to have lower EMC than pine and spruce at a given RH, so the RH/EMC pairs were adjusted accordingly for the two species of cedar: (95% RH, 18% MC); (98% RH, 22% MC); (99% RH, 30% MC); and (99.6% RH, 40% MC). The moisture storage function of Zelinka et al. (2016) was modified slightly to achieve the same shape while approaching the revised capillary saturation value.

For all three data sources, the RH-dependence of the vapor diffusion resistance factor was retained up to 90% RH, above which it was held constant, as described in Section 3. No further changes were made to the hygrothermal properties other than D_w as described below.

The experimental A-value for each wood was identified as the slope of a linear regression of water uptake vs. square root of time based on data points during the initial 24 h (or all data points if duration was less than 24 h). The regression was not forced through the origin; this provided the best overall fit to data that in some cases was non-linear.

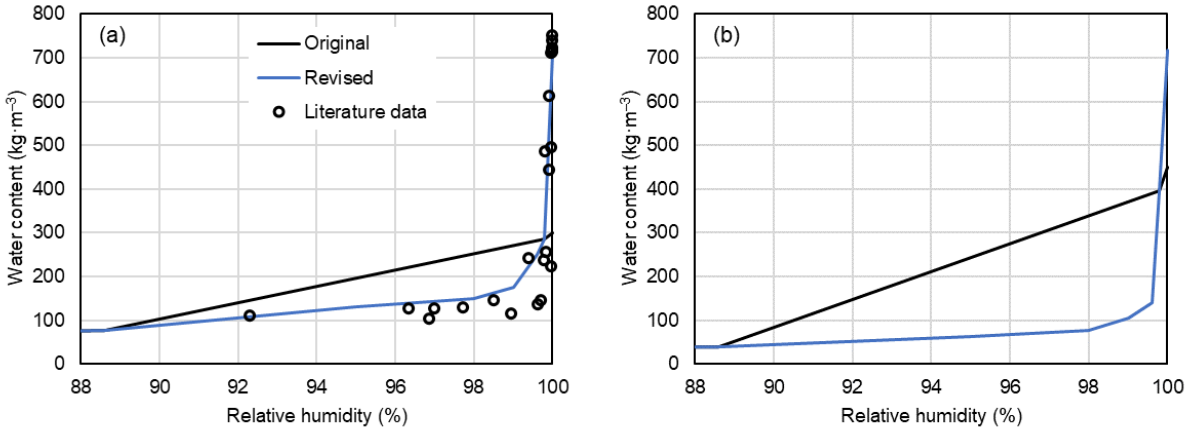

Figure 4 Original and revised moisture storage functions in the high RH range for (a) southern yellow pine and (b) western red cedar. Literature data in (a) for North American pine species from Tremblay et al. (1996), Zhang and Peralta (1999) and Wang et al. (2014).

Water uptake in each wood was simulated using WUFI software (IBP 2021). The initial condition was 50% RH and 22 °C (72 °F). The exterior boundary condition was 100% RH and "measured rain" of 5 kg·m^{-2}·h^{-1} (1 lb·ft^{-2}·h^{-1}), with a rain exposure factor of 1.0, a rain deposition factor of 1.0, and an adhering fraction of rain of 1.0 to ensure an excess supply of water like the partial immersion test. The interior boundary condition was the same as the initial condition but with a vapor barrier (s_d-value of 100 m; vapor permeance of 0.04 perm) to reflect the laboratory test, where the top surface of the specimen is covered to prevent evaporation. The liquid transport coefficient for suction (D_w) was set to a constant initial value estimated from Equation (2), beginning at the water content corresponding to 99% RH (see Section 2) up to capillary saturation. Simulated water uptake was calculated as the difference between total water content (kg·m^{-2} or lb·ft^{-2}) for each hour and the initial total water content (at time = 0). The optimal value of D_w was found by trial and error such that the slope of the simulated water uptake vs. square root of time matched the experimental A-value.

The fitting parameters k_1 and k_2 in Equation (3) were then identified as follows. Initial estimates for k_1 and k_2 were 1 and 0, respectively. The range of D_w values spanned about three orders of magnitude, so our optimization used relative errors rather than squaring the absolute errors. The relative error for each wood, e_i, was calculated as

$$e_i = \frac{D_i^{opt} - D_i^{eqn}}{D_i^{opt}} \tag{4}$$

where D_i^{opt} is the optimal value of D_w found by simulation and D_i^{eqn} is the value of D_w calculated with Equation (3). The values of k_1 and k_2 were selected that minimized the sum of $|e_i|$ over all woods.

5. RESULTS AND DISCUSSION

The liquid diffusivity values calculated with Equation (3) are compared with the optimal values found by simulation in Figure 5. The nine data sets cover a range of North American softwood species spanning three orders of magnitude in liquid diffusivity. The mean relative error is 11%; maximum relative error is 63% (eastern white cedar); and six out of nine values have relative error of 3% or less. Water absorption coefficient, capillary saturation, and vapor diffusion resistance factor at 90% RH for each data set are summarized in Table 1, together with liquid diffusivity values and relative errors. The optimized values of k_1 and k_2 in Equation (3) are 0.8336 (dimensionless) and 2.923×10^{-11} m^2·s^{-1} (1.133×10^{-6} ft^2·h^{-1}), respectively. The value of k_1 thus falls between the suggested values of $\pi/4$ (≈0.785) and 1 (see Section 3).

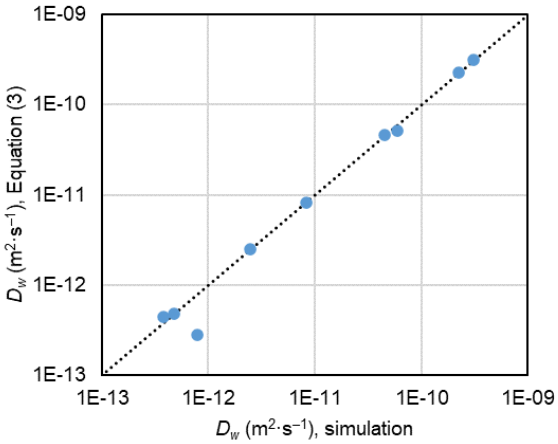

Figure 5 Log-log plot of liquid diffusivity values for nine woods calculated with Equation (3) vs. values optimized by simulation. The dotted line indicates $y = x$.

Table 1. Liquid Diffusivity and Related Properties of Various Woods

Wood Species[a]	Reference	A, kg·m^{-2}·s$^{-0.5}$ (lb·ft^{-2}·h$^{-0.5}$)	w_c, kg·m^{-3} (lb·ft^{-3})	μ(90)	D_w, m^2·s^{-1} (ft^2·h^{-1}) Simulation	D_w, m^2·s^{-1} (ft^2·h^{-1}) Equation (3)	$\lvert e_i \rvert$
E. white cedar	Kumaran et al. (2002)	0.0015 (0.018)	739 (46.2)	10.0	7.8×10^{-13} (3.0×10^{-8})	2.9×10^{-13} (1.1×10^{-8})	0.63
W. red cedar		0.0007 (0.009)	718 (44.9)	90.9	3.8×10^{-13} (1.5×10^{-8})	4.4×10^{-13} (1.7×10^{-8})	0.17
E. white pine		0.0050 (0.061)	658 (41.1)	20.4	4.5×10^{-11} (1.7×10^{-6})	4.6×10^{-11} (1.8×10^{-6})	0.03
SYP		0.0117 (0.144)	711 (44.4)	12.3	2.2×10^{-10} (8.5×10^{-6})	2.2×10^{-10} (8.5×10^{-6})	0.002
Spruce		0.0019 (0.023)	796 (49.8)	7.1	4.8×10^{-13} (1.9×10^{-8})	4.8×10^{-13} (1.9×10^{-8})	<0.001
SYP, radial	Zelinka et al. (2016)	0.0127 (0.156)	652 (40.8)	7.5	3.1×10^{-10} (1.2×10^{-5})	3.1×10^{-10} (1.2×10^{-5})	0.005
SYP, tangential		0.0053 (0.065)	652 (40.8)	14.0	6.0×10^{-11} (2.3×10^{-6})	5.2×10^{-11} (2.0×10^{-6})	0.13
Douglas-fir	Kordziel et al. (2020)	0.0021 (0.026)	887 (55.4)	14.0	2.5×10^{-12} (9.7×10^{-8})	2.5×10^{-12} (9.7×10^{-8})	<0.001
Spruce-pine-fir		0.0026 (0.032)	702 (43.9)	9.3	8.3×10^{-12} (3.2×10^{-7})	8.1×10^{-12} (3.1×10^{-7})	0.02

[a] E.: eastern; W.: western; SYP: southern yellow pine

The impact of the improved liquid diffusivity on simulated water uptake is shown in Figure 6 for two examples. In Figure 6a the revised simulation using Equation (3) is compared with measured data for spruce (Kumaran et al. 2002) and simulations using the original properties in the WUFI North America Database. In this case the measurement duration was approximately 7.1 hours. In Figure 6b the simulations are compared with measurements for Douglas-fir (Kordziel et al. 2020), for which the duration was approximately 594 hours (nearly 25 days). In this case the original simulation uses the liquid diffusivity approach of Equation (1) while the revised simulation uses Equation (3). In both examples, the revised simulations compare favorably with measurements.

The approximation method for liquid diffusivity in wood presented in this paper has several advantages: (a) it partitions liquid and vapor transport in a way that more closely aligns with the current understanding of wood–water interactions, thus avoiding double counting and improving simulation accuracy; (b) it is practical and efficient to implement in hygrothermal models; (c) it is applicable to a broad range of North American softwoods; and (d) liquid diffusivity can be calculated directly from the water absorption coefficient, capillary saturation value, and vapor diffusion resistance factor, so the method does not require moisture profile measurements or additional drying experiments.

Several limitations of this study need to be mentioned. For most of the wood species, the literature data did not include measured capillary saturation values, so we relied on estimated values. In addition, the moisture storage function at high RH did not have enough data points to give the correct shape, so we inserted values based on other literature data. Our approach aimed to give a practical approximation rather than a detailed description of complexities such as non-linear water uptake vs.

square root of time.

The two wood species with the largest relative errors in fitting Equation (3) were eastern white cedar and western red cedar. These species may behave differently from other softwoods and require different fitting parameters. Further investigation of a broader range of wood species would be needed to justify different groupings of wood species.

We also recommend further measurements of capillary saturation, equilibrium moisture content in the high RH range, moisture profiles during the water absorption process, and drying experiments. Although the scope of this study was restricted to modeling water absorption, we recommend investigating whether the approximation method developed here could be extended for modeling liquid transport during drying and redistribution. Finally, given the appreciable inherent variation in properties within any wood species, sensitivity analysis is recommended to counter the risk of underpredicting water absorption in hygrothermal simulations.

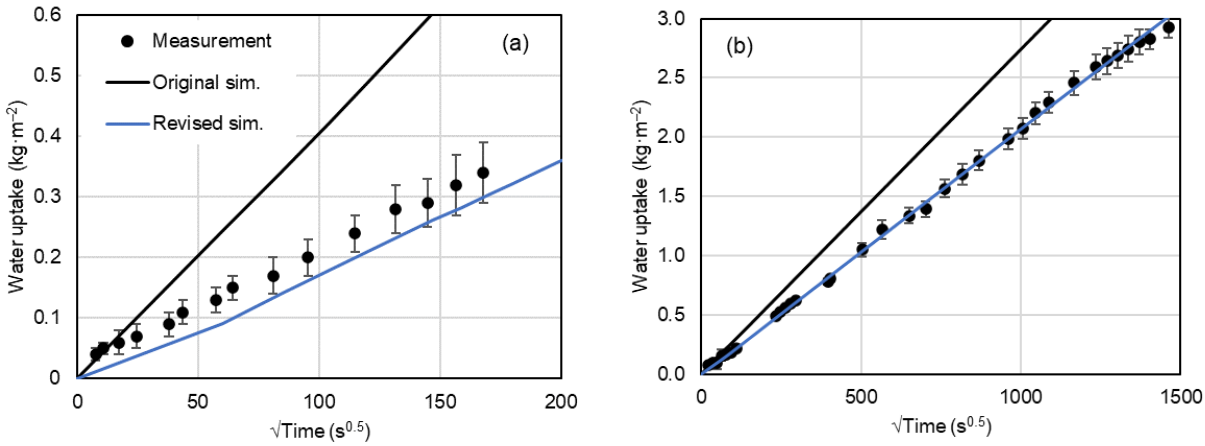

Figure 6 Comparison of water absorption measurements and simulations: (a) data for spruce (Kumaran et al. 2002), original simulation using properties from the WUFI North America Database (IBP 2021), and revised simulation using liquid diffusivity from Equation (3); (b) data for Douglas-fir (Kordziel et al. 2020), original simulation using Equation (1), and revised simulation using Equation (3). Note the different horizontal and vertical axis scales.

6. CONCLUSIONS

This paper presents an improved approximation method for modeling liquid water absorption in wood. This method directly addresses the partitioning between vapor and liquid transport in hygrothermal models. Prior approaches overpredict the rate of water absorption in wood because vapor diffusion is incorrectly assumed to be negligible during the water uptake measurement and is thus double counted in the simulation. Drawing on the current understanding of wood-water interactions, we argue that 99% RH is a reasonable threshold for capillary water transport and that an RH-dependent vapor diffusion resistance factor is a practical representation of combined diffusion of cell wall water and water vapor in the pore structure. Our approach for calculating liquid diffusivity builds on earlier approximations. For a given wood species, a single liquid diffusivity value is calculated based on the measured water absorption coefficient, capillary saturation value, and vapor diffusion resistance factor at 90% RH. The method uses two fitting parameters that are optimized across a range of North American softwood species from the literature using one-dimensional simulations. Liquid diffusivity values span three orders of magnitude with a mean relative error of 11%. This practical approach improves simulation accuracy and does not require additional data beyond ordinary hygrothermal property measurements. Further work is recommended to test the approach with a broader set of experimental data, to investigate outliers, and to understand differences between wood species.

REFERENCES

ASTM. 2019. ASTM C1794-19, Standard Test Methods for Determination of the Water Absorption Coefficient by Partial Immersion. West Conshohocken, PA: ASTM International.

Carmeliet, J., Janssen, H., and H. Derluyn. 2007. An improved moisture diffusivity model for porous building materials. In *Proceedings of 12th Symposium for Building Physics*, Dresden, Germany.

Chen, M., Coasne, B., Guyer, R., Derome, D., and J. Carmeliet. 2018. Role of hydrogen bonding in hysteresis observed in sorption-induced swelling of soft nanoporous polymers. *Nature Communications* 9(1): 3507. https://doi.org/10.1038/s41467-018-05897-9

Engelund, E.T., Thygesen, L.G., and P. Hoffmeyer. 2010. Water sorption in wood and modified wood at high values of relative humidity. Part 2: Appendix. Theoretical assessment of the amount of capillary water in wood microvoids. Holzforschung 64(3): 325–330. https://doi.org/10.1515/hf.2010.061

Fortin, Y. 1979. *Moisture content-matric potential relationship and water flow properties of wood at high moisture contents*. Ph.D. dissertation. Vancouver, Canada: University of British Columbia, Department of Forestry.

Fredriksson, M. 2019. On wood–water interactions in the over-hygroscopic moisture range—mechanisms, methods, and influence of wood modification. *Forests* 10(9): 779. https://doi.org/10.3390/f10090779

Fredriksson, M., and E.E. Thybring. 2019. On sorption hysteresis in wood: Separating hysteresis in cell wall water and capillary water in the full moisture range. *PLoS ONE* 14(11): e0225111. https://doi.org/10.1371/journal.pone.0225111

Gezici-Koç, Ö., Erich, S.J.F., Huinink, H.P., van der Ven, L.G.J., and O.C.G. Adan. 2017. Bound and free water distribution in wood during water uptake and drying as measured by 1D magnetic resonance imaging. *Cellulose* 24: 535–553. https://doi.org/10.1007/s10570-016-1173-x

IBP. 2021. WUFI® Pro, version 6.5.3. Holzkirchen, Germany: Fraunhofer Institute for Building Physics. https://wufi.de/en/

ISO. 2002. ISO 15148:2002, Hygrothermal Performance of Building Materials and Products—Determination of Water Absorption Coefficient by Partial Immersion. Geneva: International Organization for Standardization.

Jakes, J.E., Hunt, C.G., Zelinka, S.L., Ciesielski, P.N., and N.Z. Plaza. 2019. Effects of moisture on diffusion in unmodified wood cell walls: A phenomenological polymer science approach. *Forests* 10(12): 1084. https://doi.org/10.3390/f10121084

Kordziel, S., Glass, S.V., Boardman, C.R., Munson, R.A., Zelinka, S.L., Pei, S., and P.C. Tabares-Velasco. 2020. Hygrothermal characterization and modeling of cross-laminated timber in the building envelope. *Building and Environment* 177: 106866. https://doi.org/10.1016/j.buildenv.2020.106866

Kulasinski, K., Guyer, R., Derome, D., and J. Carmeliet. 2015. Water diffusion in amorphous hydrophilic systems: A stop and go process. *Langmuir* 31(39): 10843–10849. https://doi.org/10.1021/acs.langmuir.5b03122

Kumaran, M.K. 1999. Moisture diffusivity of building materials from water absorption measurements. *Journal of Thermal Envelope and Building Science* 22(4): 349–355. https://doi.org/10.1177/109719639902200409

Kumaran, M.K., Lackey, J.C., Normandin, N., Tariku, F., and D. van Reenen. 2002. *A thermal and moisture transport property database for common building and insulating materials*. Final Report, ASHRAE Research Project 1018-RP. Atlanta: ASHRAE.

Künzel, H.M. 1995. Simultaneous heat and moisture transport in building components: one- and two-dimensional calculation using simple parameters. Stuttgart: Fraunhofer IRB Verlag.

Krus, M. 1996. Moisture transport and storage coefficients of porous mineral building materials: Theoretical principles and new test methods. Stuttgart: Fraunhofer IRB Verlag.

Krus, M., and H.M. Künzel. 1993. Determination of Dw from A-value. *IEA Annex XXIV Report T3-D-93/02*.

Krus, M., and T.A. Vik. 1999. Determination of hygric material properties and calculation of the moisture balance of wooden prisms. In *5th Symposium on Building Physics in the Nordic Countries*, Gothenburg, Sweden, August 24-26, 1999.

Nopens, M., Wadsö, L., Ortmann, C., Fröba, M., and A. Krause. 2019. Measuring the heat of interaction between lignocellulosic materials and water. *Forests* 10: 674. https://doi.org/10.3390/f10080674

Plaza, N.Z. 2019. On the experimental assessment of the molecular-scale interactions between wood and water. *Forests* 10: 616. https://doi.org/10.3390/f10080616

Sandberg, K., and J.-G. Salin. 2012. Liquid water absorption in dried Norway spruce timber measured with CT scanning and viewed as a percolation process. *Wood Science and Technology* 46: 207–219. https://doi.org/10.1007/s00226-010-0371-1

Sedighi-Gilani, M., Griffa, M., Mannes, D., Lehmann, E., Carmeliet, J., and D. Derome. 2012. Visualization and quantification of liquid water transport in softwood by means of neutron radiography. *International Journal of Heat and Mass Transfer* 55(21–22): 6211–6221. https://doi.org/10.1016/j.ijheatmasstransfer.2012.06.045

Stone, J.E., and A.M. Scallan. 1967. The effect of component removal upon the porous structure of the cell wall of wood. II. Swelling in water and the fiber saturation point. *Tappi* 50(10): 496–501.

Thybring, E.E., Glass, S.V., and S.L. Zelinka. 2019. Kinetics of water vapor sorption in wood cell walls: state of the art and research needs. *Forests* 10: 704. https://doi.org/10.3390/f10080704

Thygesen, L.G., Engelund, E.T., and P. Hoffmeyer. 2010. Water sorption in wood and modified wood at high values of relative humidity. Part I: Results for untreated, acetylated, and furfurylated Norway spruce. *Holzforschung* 64(3): 315–323. https://doi.org/10.1515/hf.2010.044

Tremblay, C., Cloutier, A., and Y. Fortin. 1996. Moisture content–water potential relationship of red pine sapwood above the fiber saturation point and determination of the effective pore size distribution. *Wood Science and Technology* 30(5): 361–371. https://doi.org/10.1007/BF00223556

Wang, J.Y., Mukhopadhyaya, P., and P.I. Morris. 2014. Sorption and capillary condensation in wood and the moisture content of red pine. *Journal of Building Physics* 37(4): 327–347. https://doi.org/10.1177/1744259112453829

Zelinka, S.L., Lambrecht, M.J., Glass, S.V., Wiedenhoeft, A.C., and D.J. Yelle. 2012. Examination of water phase transitions in Loblolly pine and cell wall components by differential scanning calorimetry. *Thermochimica Acta* 533: 39–45. https://doi.org/10.1016/j.tca.2012.01.015

Zelinka, S.L., Glass, S.V., Boardman, C.R., and D. Derome. 2016. Moisture storage and transport properties of preservative treated and untreated southern pine wood. *Wood Material Science and Engineering* 11(4): 228–238. https://doi.org/10.1080/17480272.2014.973443

Zhang, J., and P.N. Peralta. 1999. Moisture content-water potential characteristic curves for red oak and loblolly pine. *Wood and Fiber Science* 31(4): 360–369.

Zillig, W. 2009. *Moisture transport in wood using a multiscale approach*. Ph.D. dissertation. Leuven, Belgium: Katholieke Universiteit Leuven.